HIGH-PRESSURE VIBRATING PRESSURE TRANSDUCER

Elbert M. Moffatt

Hamilton Standard

Prepared for:

Army Air Mobility Research and Development Laboratory

November 1972

USAAMRDL TECHNICAL REPORT 72-42

HIGH-PRESSURE VIBRATING PRESSURE TRANSDUCER

By

E. M. Moffatt

November 1972

EUSTIS DIRECTORATE
U. S. ARMY AIR MOBILITY RESEARCH AND DEVELOPMENT LABORATORY
FORT EUSTIS, VIRGINIA

CONTRACT DAAJ02-71-C-0067
HAMILTON STANDARD DIVISION
UNITED AIRCRAFT CORPORATION
WINDSOR LOCKS, CONNECTICUT

DISCLAIMERS

The findings in this report are not to be construed as an official Department of the Army position unless so designated by other authorized documents.

When Government drawings, specifications, or other data are used for any purpose other than in connection with a definitely related Government procurement operation, the United States Government thereby incurs no responsibility nor any obligation whatsoever; and the fact that the Government may have formulated, furnished, or in any way supplied the said drawings, specifications, or other data is not to be regarded by implication or otherwise as in any manner licensing the holder or any other person or corporation, or conveying any rights or permission, to manufacture, use, or sell any patented invention that may in any way be related thereto.

Trade names cited in this report do not constitute an official endorsement or approval of the use of such commercial hardware or software.

DISPOSITION INSTRUCTIONS

Destroy this report when no longer needed. Do not return it to the originator.

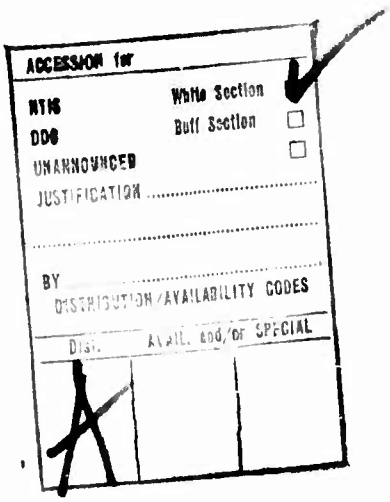

UNCLASSIFIED

Security Classification

DOCUMENT CONTROL DATA - R & D

(Security classification of title, body of abstract and indexing annotation must be entered when the overall report is classified)

1. ORIGINATING ACTIVITY (Corporate author) Hamilton Standard Division United Aircraft Corporation Windsor Locks, Connecticut	2a. REPORT SECURITY CLASSIFICATION Unclassified 2b. GROUP

3. REPORT TITLE

HIGH-PRESSURE VIBRATING PRESSURE TRANSDUCER

4. DESCRIPTIVE NOTES (Type of report and inclusive dates)

Final

5. AUTHOR(S) (First name, middle initial, last name)

Elbert M. Moffatt

6. REPORT DATE	7a. TOTAL NO. OF PAGES	7b. NO. OF REFS
November 1972	~~47~~ 49	-

8a. CONTRACT OR GRANT NO.	9a. ORIGINATOR'S REPORT NUMBER(S)
DAAJ02-71-C-0067 b. PROJECT NO. Task 1F162203A43405 c. d.	USAAMRDL Technical Report 72-42 9b. OTHER REPORT NO(S) (Any other numbers that may be assigned this report) None

10. DISTRIBUTION STATEMENT

Approved for public release; distribution unlimited.

11. SUPPLEMENTARY NOTES	12. SPONSORING MILITARY ACTIVITY
N/A Details of illustrations in this document may be better studied on microfiche.	Eustis Directorate U. S. Army Air Mobility Research & Development Laboratory Ft. Eustis, Virginia

13. ABSTRACT

This report describes the modifications and testing done to develop a high-pressure version of the vibrating cylinder pressure transducer previously developed at Hamilton Standard Division. The previous designs of this device were rated at 20 and 50 psia maximum pressure and -65°F to 250°F operating temperature. The modification is rated at 250 psia and -65°F to 200°F. In addition, the results of a company project to develop a modification for higher temperatures (up to 400°F) are reported.

The vibrating cylinder pressure is an extremely accurate device which is currently being used in the air inlet control of the F-15 aircraft. In comparison with other transducers, its superiority is in the elimination of hysteresis errors, minimizing of drift errors, immunity to external vibration, very high resolution, and digital output which minimizes interface errors. It is small and light and has no moving parts aside from the vibrating member, so its life is indefinitely long.

DD FORM 1 NOV 68 1473 REPLACES DD FORM 1473, 1 JAN 64, WHICH IS OBSOLETE FOR ARMY USE.

I-a

UNCLASSIFIED

Security Classification

14. KEY WORDS	LINK A		LINK B		LINK C	
	ROLE	WT	ROLE	WT	ROLE	WT
pressure pressure sensor sensor vibrating cylinder sensor transducer						

DEPARTMENT OF THE ARMY
U. S. ARMY AIR MOBILITY RESEARCH & DEVELOPMENT LABORATORY
EUSTIS DIRECTORATE
FORT EUSTIS, VIRGINIA 23604

As a portion of this Directorate's continuing program to support research and development efforts on aircraft diagnostic and inspection equipment, this contract was undertaken to modify and test a pressure sensor that would result in an improved pressure sensor for diagnostic applications.

An advanced type of low-pressure transducer that had previously been developed by the contractor uses a vibrating cylinder as the basic transducing element with an electronic driver element. This program was to expand the pressure-sensing capability by redesigning the existing transducer so that it could be used to sense the higher pressures necessary for engine diagnostic applications. The effort demonstrated the ability of the pressure sensor to accurately measure pressures up to 250 psig.

The technical monitor for this program was Mr. G. William Hogg, Military Operations Technology Division.

I-C

Task 1F162203A43405
Contract DAAJ02-71-C-0067
USAAMRDL Technical Report 72-42
November 1972

HIGH-PRESSURE VIBRATING PRESSURE TRANSDUCER

Final Report

By
E. M. Moffatt

Prepared by

Hamilton Standard Division
United Aircraft Corporation
Windsor Locks, Connecticut

for

EUSTIS DIRECTORATE
U. S. ARMY AIR MOBILITY RESEARCH AND DEVELOPMENT LABORATORY
FORT EUSTIS, VIRGINIA

II

SUMMARY

This report describes the modifications and testing done to develop a high-pressure version of the vibrating cylinder pressure transducer previously developed at Hamilton Standard Division.

The previous designs of this device were rated at 20 and 50 psia maximum pressure and -65°F to 250°F operating temperature. The modification is rated at 250 psia and -65°F to 200°F.

In addition, the results of a company project to develop a modification for higher temperatures (up to 400°F) are reported.

TABLE OF CONTENTS

LIST OF ILLUSTRATIONS

LIST OF TABLES

LIST OF SYMBOLS

a	cylinder radius, in.
b	width of vibrating section, in.
c	length of vibrating section, in.
d_1	density of cylinder wall, lb/in.^{3}
d_2	density of gas, lb/in.^{3}
E	elastic modulus of cylinder, lb/in.^{2}
f	frequency, Hz
fo	zero pressure frequency, Hz
h	cylinder wall thickness, in.
K_1	spring constant of cylinder wall, lb/in.
K_2	pressure constant of cylinder wall, in.-lb
K_3	gas density constant of cylinder wall, in.^{3}/lb
l	cylinder length, in.
m	cylinder vibration mode, parallel to axis
M_e	equivalent mass of cylinder wall
n	cylinder vibration mode, circumferential
p	pressure differential across cylinder wall, lb/in.^{2}
p_a	absolute pressure, lb/in.^{2}
p_m	maximum pressure differential, lb/in.^{2}
S_t	tensile stress, lb/in.^{2}
t	period of vibration, microseconds
t_0	corrected period, microseconds
T	absolute temperature, °R

T_f	temperature, °F
T_0	reference temperature, °R
Δt	correction to period, microseconds
V	diode voltage, volts

1.0 INTRODUCTION

The vibrating cylinder pressure transducer is an extremely accurate device which is currently being used in the air inlet control of the F-15 aircraft. Its configuration is shown in Figure 1.

In comparison with other transducers, its superiority is in the elimination of hysteresis errors, minimizing of drift errors, immunity to external vibration, very high resolution and digital output which minimizes interface errors. It is small and light and has no moving parts aside from the vibrating member, so its life is indefinitely long.

2.0 THEORY OF OPERATION

2.1 Basic Vibration Modes

Its principle of operation is illustrated in Figure 2. Its sensing element is a thin-walled metal cylinder which is excited into a certain mode of vibration by an electromagnet (A) located inside with its poles in close proximity to the cylinder wall. The vibration is sensed by a second electromagnet (B).

The mode of vibration is illustrated in Figure 2. It consists of a radial deformation of the cylinder walls which creates axial nodes on the cylinder wall. The mode illustrated is characterized by two full "wavelengths"; i.e., the deformation is wave-like in a radial section and has crests and troughs outside and inside the mean circle. This wave motion is an oscillating one. In the mode illustrated in Figure 2, the cylinder is shown at two instants. The full line shows one shape and the dashed line the shape one-half a cycle later. These shapes intersect at four points, which lie on the mean circle and define four nodes. The cylinder can be made to vibrate, theoretically, in an infinite number of modes characterized by different values of (n). In addition to these modes, there is another set of vibration modes characterized by the shape of the cylinder wall in a cross-section parallel to the axis (as in the upper view of Figure 2). The wall is fixed at the two ends and deflects like a beam in this section. A simple deflection which is maximum at the center is identified as ($m = 1$). It can also deflect in an infinite number of other modes characterized by one more node at the center ($m = 2$), two more nodes ($m = 3$), etc. All the m values above 1 are high-frequency modes which are difficult to excite and have no desirable characteristics for a pressure sensor, so they can be ignored, and it will be assumed below that $m = 1$ for all modes.

2.2 Zero Pressure Frequency

When the cylinder is unpressurized, i.e., when the pressure is the same inside and outside, the natural frequency in any mode is dependent only on the stiffness and mass of the cylinder wall and can be expressed as:

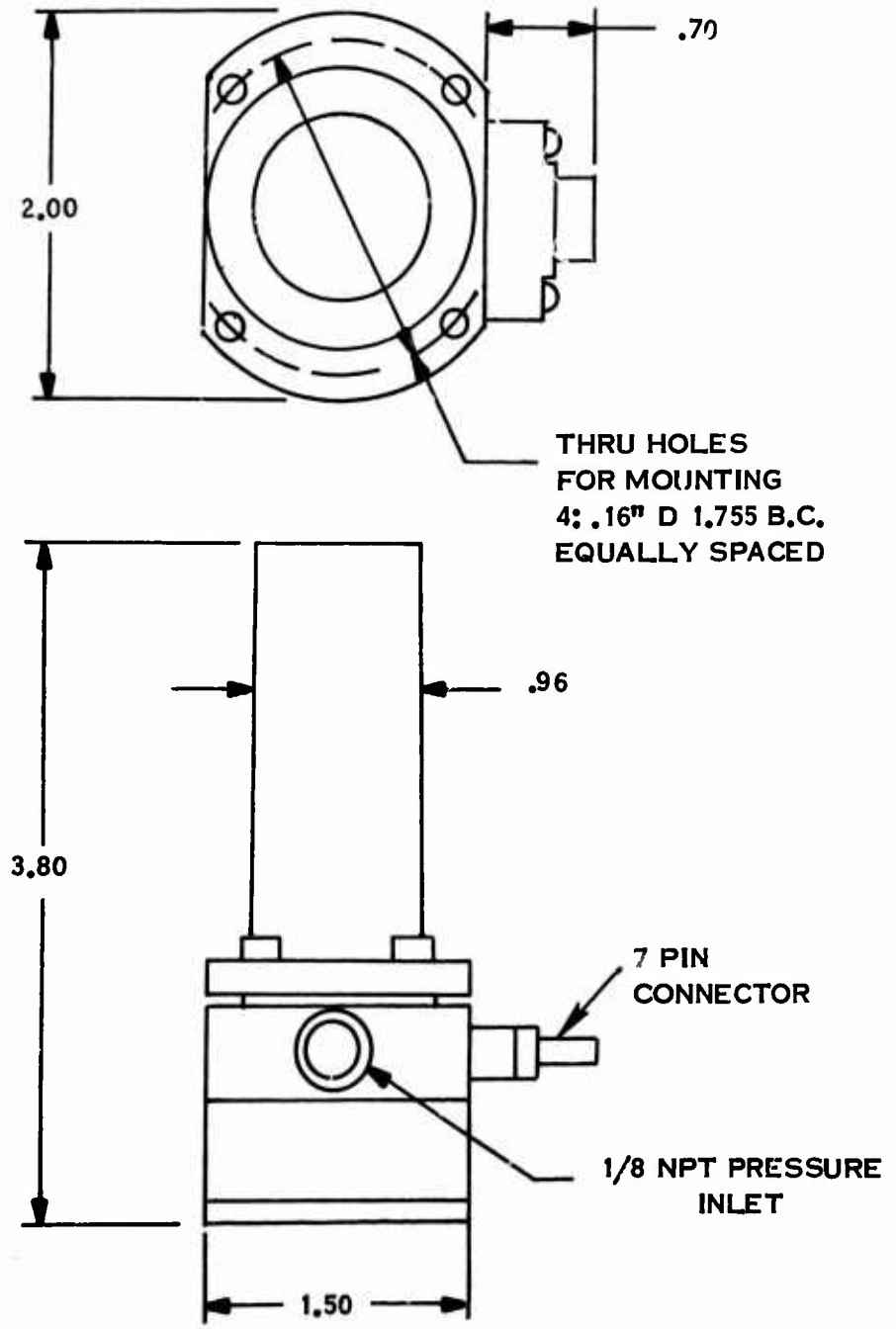

Figure 1. Installation Diagram.

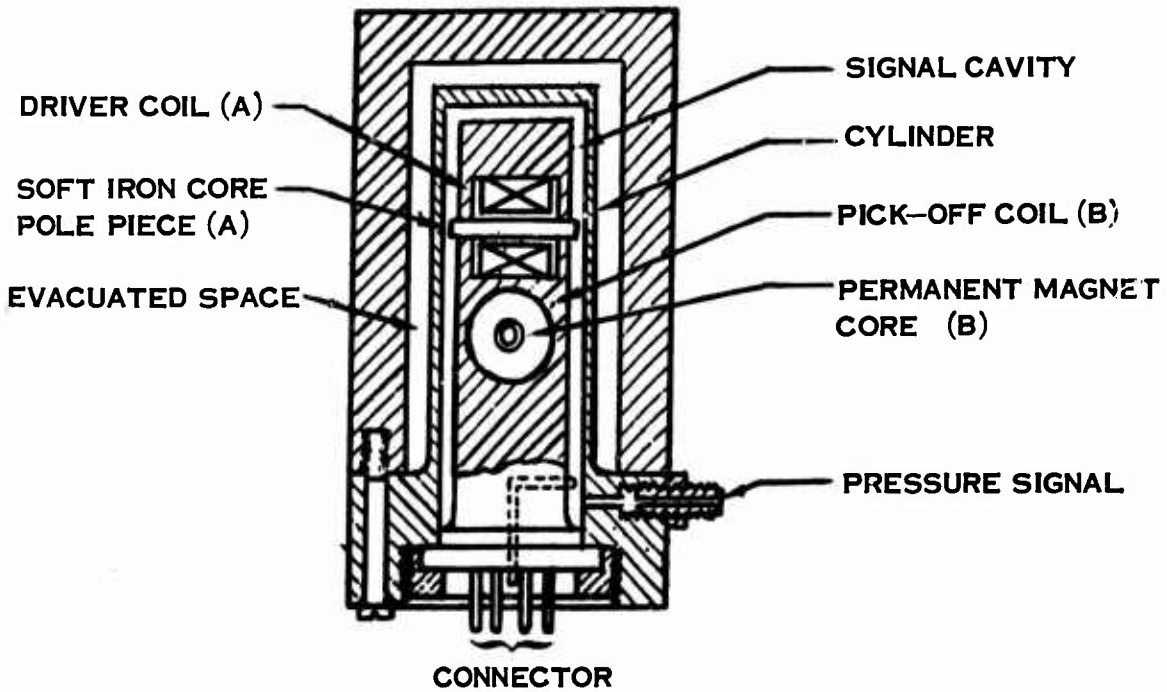

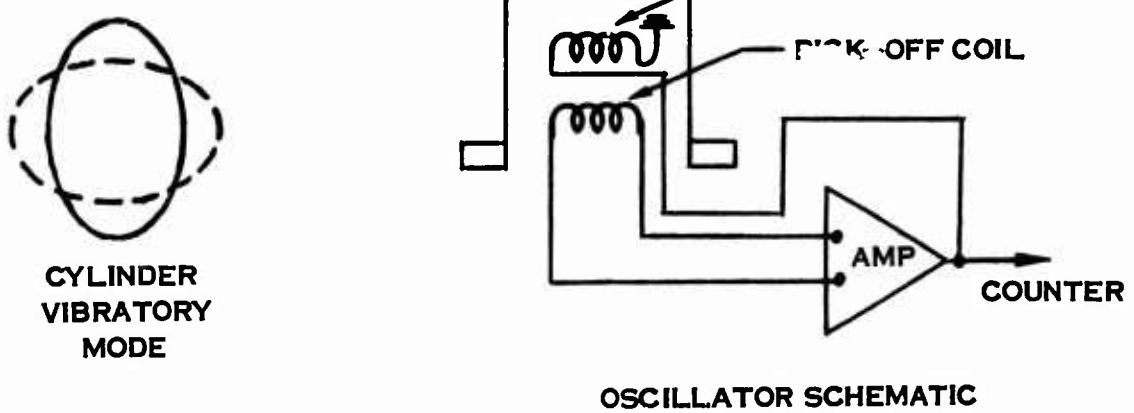

Figure 2. Construction and Operating Principle of Vibrating Cylinder Pressure Transducer.

$$f_o = K\sqrt{K_1/M_e} \qquad (1)$$

where f_o = zero pressure frequency

K_1 = spring constant of wall

M_e = equivalent mass of wall

K = constant appropriate for dimensions

The spring constant, K_1, is due to the stiffness of each section of the wall between two axial nodes. Each of these sections can be considered as a curved plate freely supported on all four sides. For a simple beam, this stiffness is

$$K_1 = KE\ b\ h^2/c^3 \qquad (2)$$

where E = elastic constant of material

h = thickness

b = width

c = length between supports

Since this is a curved plate, the stiffness depends simultaneously on bending about two axes at right angles to each other, and the curvature R affects the stiffness for one axis; so the exact equation for K_1 is more complicated, but it can be seen that it will depend directly on E and h^2 and in a more complex way on width and length on each axis. The width and length factors are completely defined by

l = cylinder length

a = cylinder radius

n = vibration mode

The effective mass, M_e, in Eq. 1 above is chiefly a function of wall thickness (h) and metal density (d_1). Since this appears in the denominator and h^2 appears in the numerator as a parameter of stiffness (K_1 in Eq. 2), the overall effect of wall thickness on frequency is approximately $\sqrt{h}$. For a simple beam or flat plate, the distance between nodes determines the length c; and since the stiffness varies as $1/c^3$, the frequency would go up as the number of nodes increase and c decreases, so the lowest frequency mode would be the one with the lowest number of nodes. For a curved plate, the stiffness in bending about an axis perpendicular to the axis of curvature also depends on the angle subtended at the center of curvature by the curved

width, increasing as this angle increases, so this stiffness increases as the number of nodes decrease. Since this effect is opposite to the first effect, it turns out that the lowest frequency is not necessarily the one with the fewest nodes. The lowest number of nodes is for n = 2 for a vibration excited by two forces acting 180° apart simultaneously (the magnetic forces at the two ends of the exciting magnet), but for most cylinder geometries the (n = 4) mode has the lowest natural frequency and largest amplitude and is the one selected for operation as a pressure sensor.

2.3 Electrical Drive Circuitry

To ensure operation in this mode, the electrical design provides the proper phase shift between sensed motion and forced motion. Figure 2 shows that the voltage generated by motion is sensed by the pick-off coil and fed into an amplifier, which includes the proper phase shift and supplies drive voltage to the driver coil.

Since no external frequency is supplied to the amplifier, the drive frequency can vary freely and will always adjust itself to the natural frequency of the cylinder.

When the power is turned on initially, the cylinder is at rest, but electrical noise inherent to the amplifier will create small random pulses in the driver coil. These, in turn, make the cylinder "ring" at its natural frequency at low amplitude. These small deflections are sensed by the pick-off coil and amplified and fed back to drive the cylinder, so it rapidly builds up to a high-amplitude resonant vibration.

The maximum drive voltage is limited to a fixed value, so the maximum deflection can never exceed a fixed value. The actual pick-off voltage varies with temperature and pressure of operation. The upper temperature limit is set by a combination of temperature effect on gain of the amplifier and on the magnetic properties of the cylinder.

2.4 Frequency vs. Pressure Effects

The pressure-sensing property of a vibrating cylinder is due to hoop tension generated in the cylinder wall by a gas pressure differential between the outside and inside of the cylinder. An evacuated space is provided between the vibrating cylinder and an outer cylinder as shown in Figure 2. For this design, then, the pressure differential is equal to the absolute pressure of the gas.

The tension effect in the cylinder wall can be visualized if the wall is considered to be a limp membrane with zero stiffness. If a membrane is stretched, it can resist a pressure and its deflection depends on the tension as well as the pressure. The tension then is similar to a spring constant, so the frequency equation above becomes

$$f = K\sqrt{[K_1 + K_2 (p)]/M_e} \qquad (3)$$

where K_2 = constant depending on geometry

p = pressure differential

Pressure is related to tension in the cylinder wall by

$$p\,a = s$$

where a = cylinder radius

s = tension, lb/in.

The equation above indicates that the measured frequency is some constant value at zero pressure and increases with pressure.

Frequency is measured by amplifying the output of the amplifier (Figure 2) and clipping it to give a square wave with a very fast rise time. This is used to gate a counter. The counter can be gated in two ways to give either frequency or period.

2.4.1 Frequency Measurement

If the counter is gated by its own internal clock for, say, 1 second, it can count the number of cycles produced by the transducer in this period, and this is equal to the frequency (cycles/sec.). Since it can count only once for each zero cross-over in a given direction of the square wave from the transducer, it cannot count fractional cycles; hence, if it is gated for 1 second, its accuracy is $\pm$ 1 Hz. If the gating period is increased to 10 or 100 seconds, the accuracy is increased to 0.1 Hz or 0.01 Hz.

The transducers normally operate in the range of 5000 to 8000 Hz, and the frequency change from zero to full pressure is about 1000 to 1500 Hz, so an accuracy of $\pm$1 Hz is only 0.1% on resolution. Since the transducer accuracy is about ten times this high, a gating period of 10 seconds would be the minimum to give 0.01% resolution and take advantage of the inherent accuracy.

2.4.2 Period Measurement

If the counter internal clock operates at 10 megahertz and this is used to drive the counter while the transducer signal is used to gate the counter, a period of 1/5000 second, corresponding to one cycle at 5000 Hz, would give a count of 2000 (10,000,000 /5000). If the frequency range for full-scale pressure is 1000

Hz, the count range would be 400 and an accuracy of ±1 would give a resolution of 1/400 = 0.25%. To get a resolution of 0.01%, the gating period can be increased to 25 transducer cycles or 1/200 second (25/5000).

By measuring period (t) instead of frequency (f), then, the counting time is reduced from 10 seconds to 1/200 second for the same resolution of 0.01%, so it is obviously more desirable to calibrate the transducer in terms of period than in terms of frequency, and all the equations below are based on this.

If the reciprocal of the frequency equation above (Eq. 3) is written, it can be seen that a typical calibration will show a maximum period at zero pressure and a decreasing period at higher pressures. This type of curve is shown for an actual calibration in Figure 3.

2.5 Temperature Effects on Frequency

Besides the pressure effects, the transducer is affected slightly by temperature. This acts in two different ways.

2.5.1 Temperature Constants of Metal

The elastic constant (E) of the metal in the cylinder changes with temperature, and dimensional changes occur for length, thickness, and radius (l, h, a). These effects are minimized by using a nickel-iron alloy with low temperature sensitivity.

2.5.2 Temperature-Density Effects

There is also a small effect on M_e due to gas density d_2. When the cylinder is vibrating, the gas whose pressure is being measured is filling the space between the magnet assembly and the cylinder, and the gas has to move with the wall, so its mass has to be added to the mass of the wall. The effect of this mass of vibrating gas will be less for a thick wall than for a thin one since its relative mass will be less, so the density error depends on wall thickness. The gas density effect appears as a temperature error, and the density is

$$d_2 = K_g \, p_a / T$$

where K_g = constant depending on gas composition

T = absolute temperature

p_a = absolute pressure

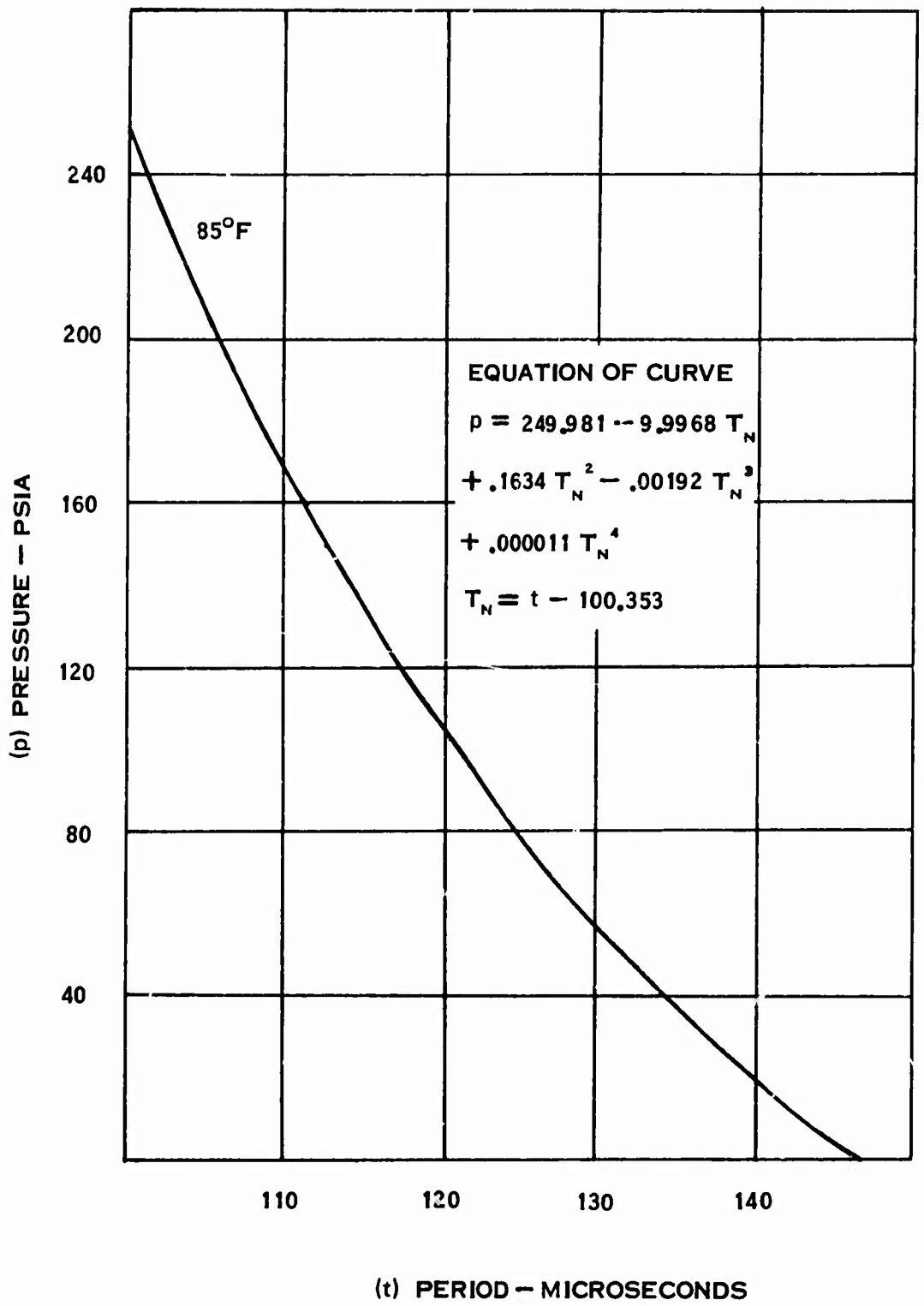

Figure 3. Pressure Versus Period Calibration at 85°F.

Since the transducer equation in general terms is

$$t = F_1 (p_a, T, d_2)$$

where F_1 = function of ( )

t = period of vibration

and $d_2 = K_g\, p_a/T = F_2 (p_a, T)$

this is equivalent to

$$t = F_3 (p_a, T)$$

In other words, gas density drops out as an explicit variable but causes an apparent temperature error.

This density effect can be minimized by the proper choice of wall thickness, but this choice also involves stress considerations and pressure sensitivity, so it is a design compromise.

2.5.3 Temperature Errors

If the temperature error is neglected, the first effect gives a zero shift since it affects zero pressure frequency. The second effect is a percent of point error since it depends on gas density, which, in turn, varies with gas pressure. Its contribution to error is zero at zero pressure since the gas has zero density at this point.

3.0 DEVELOPMENT PROGRAM

The problems were to strengthen the cylinder to stand the higher pressure without increasing the density effect excessively and to provide the proper electrical drive so that the cylinder would always vibrate in the proper mode and start oscillating at any pressure or temperature within the operating range.

The initial analytical investigation showed that the cylinder wall thickness would have to be a compromise between keeping the hoop tension within acceptable limits and still generating enough of a frequency change with pressure to give the necessary sensitivity and acceptable linearity. If this sensitivity is too low, density effects will be relatively greater.

3.1 Determining Optimum Wall Thickness for Density Effect and Linearity

The relationship between temperature and gas density effects was explained briefly in Section 2.5.2.

To see this more explicitly, Eq. 3 can be expanded.

The effective density M_e, which determines natural frequency, is a density per unit area since K_2 (p) is a force per unit area per unit deflection.

The major contribution to this term is the mass of the cylinder wall. If this has a mass per unit volume of d_1, its mass per unit area is $(d_1 h)$ where h is wall thickness.

A minor contribution is the mass of the layer of gas which vibrates with the wall. Its effective mass per unit area is $(d_2 h_2)$, where d_2 is gas density per unit volume and h_2 is the thickness of the trapped layer.

M_e is then equal to

$$M_e = d_1 h + d_2 h_2$$

$$= d_1 h \, (1 + K_3 d_2) \qquad (4)$$

where

$$K_3 = h_2/d_1 h \qquad (5)$$

If this is substituted in Eq. 3 and brought outside the radical, the result to a very close approximation is

$$f = K\sqrt{[K_1 + K_2 \, (p)]/d_1 h} \; [1 - \tfrac{1}{2} K_3 K_g p_a/T_0 + \tfrac{1}{2} K_3 K_g p_a/T_0 \; (dT/T_0)] \qquad (6)$$

where $d_2 = K_g p_a/T$

T_0 = reference temperature

dT = temperature deviation from reference

If the transducer is an absolute pressure unit, the value of p (differential pressure) inside the radical of Eq. 6 will equal p_a (absolute pressure). The frequency as determined by the radical plus the first two terms in the bracket is a function only of p_a (plus various constants), and the density effect is all contained in the third term in the brackets. This term contains p_a and temperature T expressed as a deviation dT from a reference temperature T_0.

Since both p_a and T are operating parameters, they cannot be altered, and the only design factor that can be varied to minimize the effect is K_3.

To minimize K_3, Eq. 5 shows that h_2 should be decreased or d_1 or h

increased. Since d_1 is a property of the metal used for construction and this must necessarily be a magnetic alloy, there is not any substitution that can be made here since all magnetic alloys have substantially the same density.

h_2 is proportioned to cylinder radius (a) so (h_2/h) is equivalent to (a/h), and this parameter in turn is a critical one in determining pressure sensitivity.

Eq. 6 shows that increasing the maximum pressure capability (p_a) will increase the relative density effect unless K_3 can be decreased in inverse ratio.

Eq. 5 shows that increasing the wall thickness (h) will decrease K_3, and to keep a constant hoop stress, h should be increased in direct proportion to p_a. A preliminary conclusion might be that h can be increased in the same ratio as p_a, so the density effect will be the same for the high pressure as for the low pressure design. This is erroneous, however, because it neglects the effect of changes in h on the primary term inside the radical of Eq. 6.

The expression inside the radical consists of a large fixed term K_1 and a smaller variable term $K_2(p)$. If $K_2(p)/K_1$ at maximum pressure decreases because of changes in h, the percent frequency change over the pressure range will decrease; but the density effect is multiplied by the whole expression inside the radical, so its magnitude with respect to the frequency change will increase, thus giving a larger percent full-scale density effect.

K_1 in Eq. 6 is a spring constant of the cylinder wall deflecting in a four-lobe radial pattern. This can be approximated as the sum of two bending modes of a curved plate about two axes perpendicular to each other, one parallel to the axis of the cylinder and the other perpendicular to this and forming a chord for the circular sector. The sum of these spring constants is approximately

$$K_1 = K_4 E\, h^2 \qquad (7)$$

K_2 is the spring constant developed by membrane stresses and is approximately

$$K_2 = K_5 l\, a \qquad (8)$$

The ratio of these constants K_2/K_1 where K_2 is evaluated at the maximum pressure for the design determines the pressure sensitivity in terms of frequency change between zero and full-scale pressure divided by zero pressure frequency. The higher this ratio K_2/K_1 is made, the less the density effect for a given value of K_3.

Eq. 6 can be rewritten to evaluate the total density effect as a function of wall thickness and maximum pressure as follows:

The second term in the bracket can be dropped since it is small and does not contribute to the density effect. The terms under the radical can be replaced approximately by the binomial expansion of the expression, dropping all but the first two terms.

This gives

$$f = K\sqrt{K_1/d_1h}\ [1 + \tfrac{1}{2}K_2(p_a)/K_1]\ [1 + \tfrac{1}{2}K_3\ p_a\ (dT/T_0)]$$

The bracketed terms can be multiplied, and the second-order cross-product dropped, and the expression can be written

$$f = K\sqrt{K_1/d_1h}\ [1 + K_6p_a\ (1 + K_7\ dT/T_0)] \qquad (9)$$

The initial multiplier ($K\ K_1/d_1h$) gives zero pressure, or minimum, frequency.

$$K_6 = \tfrac{1}{2}K_2/K_1$$

The K_6p_a term gives the percent change of frequency over the pressure range.

$$K_7 = K_3p_a/(\tfrac{1}{2}K_2p_a/K_1)$$

$$= K_3K_1/K_2$$

The $K_7\ dT/T_0$ term gives the percent full-scale density effect. Substituting into this from Eqs. 5, 7 and 8,

$$K_7 = K_4Eh^2h_2/K_5l\ a\ h$$

$$= K_8h \qquad (10)$$

The density error in pressure measurement in terms of the density effect at any pressure is equal to (K_7dT/T_0) multiplied by (K_6p_a) as shown by Eq. 9, so it is basically a percent of point type or error; i.e., its absolute magnitude is proportional to the variable being measured (p_a). Thus, it is not as serious as a fixed error which

gives large percent errors at small values of p_a.

Its magnitude is dependent on dT/T_0, but since the measured frequency is corrected for actual temperature, dT in this expression is not the difference between actual temperature and a fixed reference T_0, but is equal to the error in measuring transducer temperature. The transducer temperature is measured with a diode which has a sensitivity of 1.0 millivolt per degree F. This voltage can easily be measured to 0.1 millivolt, so the temperature can be read to 0.1°F. However, to allow some tolerance in this measurement and allow for temperature gradients, it was assumed that dT can be as much as 1.0°F.

The density effect on a low-pressure transducer was known from calibration to be 0.008% per degree F. An error analysis for all errors showed that to meet the development goal of .035% full-scale error, the density error should not be more than .015%; so from Eq. 10, it can be concluded that the wall thickness (h) should not be increased by a ratio of more than (.015/.008 = 1.87).

This gave a value of h of .0058".

After picking this value from the error analysis, the effect of this choice on the period-frequency curve had to be determined.

Eq. 9, which is an approximation, indicates that the percent frequency change is linear since it is proportional to $(K_6 p_a)$. This equation neglects second- and third-order terms in the binominal expansion which actually result in a nonlinear output. The amount of nonlinearity increases as $(K_6 p_a)$ at maximum pressure increases. For the value of h picked above, an exact calculation showed that the nonlinearity expressed as a maximum deviation from a straight line connecting the maximum and minimum pressure points would increase from 7% (for the low pressure unit) to 14%. This is an acceptable value in terms of the sensitivity at different parts of the range.

3.2 Determining Minimum Wall Thickness for Hoop Stresses

The maximum tensile stress in the walls is equal to

$$S_t = p_m \, a/h \qquad (11)$$

where S_t = tensile stress

p_m = maximum pressure differential

To keep this constant means that h would have to be increased in proportion to maximum pressure. This would be undesirable in terms of density error as demonstrated above.

Using the tentative value of .0058 in. for h, the stress S_t at 250 psia is 15,000 psi.

A test program was run on an existing low-pressure transducer by subjecting it to successively higher values of overpressure and checking the calibration after each pressure point. The first indication of micro-creep occurred at a value of 70,000 psi stress.

Based on this, the actual stress of 15,000 was taken as a satisfactory figure since it allows a safety margin of 4.6 X overpressure.

3.3 Amplifier Design

After constructing a test cylinder, it was subjected to pressure and temperature cycles and tested for starting.

Starting the oscillation is more difficult than sustaining it, and it requires more power as the pressure force increases and the wall becomes stiffer. Since electronic amplifiers lose gain at high temperature, the most critical conditions for starting are maximum pressure and temperature.

It was found that the one-stage operational amplifiers used to drive the low-pressure transducers would not start oscillation at maximum pressure and temperature, so a new one was built and constructed as a flat pack which could be mounted in the base of the transducer. This had two stages and was strapped down to give a gain of 600 over the whole temperature range with full output up to 100 KC. Its maximum output was limited to 1 volt to give a constant drive independent of signal magnitude. The necessary phase shift between pickup and drive voltage was supplied by the phase shifts in the coils and electromagnets.

4.0 CALIBRATION

4.1 Pressure & Temperature Calibration

4.1.1 Test Equipment

The testing was done with equipment shown in Figure 4.

The transducer was placed in an environmental chamber that could be heated or cooled, and transducer temperature was measured by a Copper-Constantan thermocouple attached to the base as well as by an internal diode.

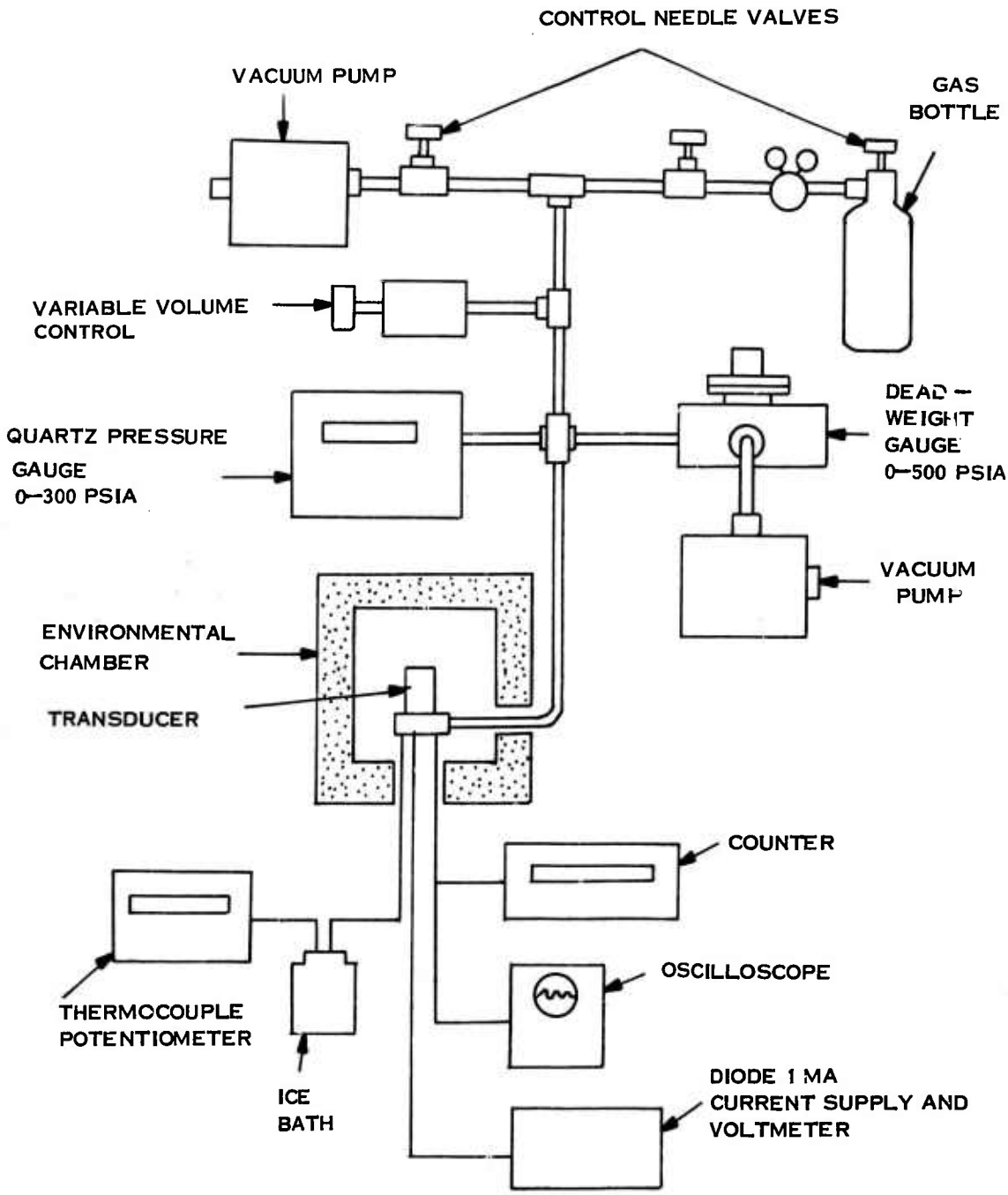

Figure 4. Calibration Test Schematic.

The thermocouple used an ice-bath cold junction, and its voltage was read on a digital voltmeter to .001 millivolt.

The diode had a fixed forward current of 1 milliamp, and the junction voltage offset was measured to indicate transducer temperature. The offset voltage was measured to .01 millivolt on a digital voltmeter.

Pressure was controlled manually by two needle valves in a Tee connecting a gas bottle with high-pressure dry air to a vacuum pump. Manipulating the valves gave pressure control over the range from 0.1 psia to 250 psia. The actual maximum pressure was limited only by the bottle pressure, but in practice it was limited to 250 psia.

The pressure was measured by a quartz helical Bourdon tube manometer which could be read to .01 psi over the whole range of .01 to 250 psia and a deadweight gauge which could be used from 25 to 300 psia. The deadweight gauge was used to calibrate the quartz manometer initially and the manometer used for the actual transducer calibration.

To get a precise pressure setting, the needle valves were adjusted to bleed gas in or out of the transducer line; when the pressure was very close to the desired value, the valves were shut off, making the transducer part of a sealed volume. A screw-actuated piston (variable volume control) was then manually adjusted to give the precise pressure required.

Transducer output was monitored with an oscilloscope to display pickup and drive voltages and a digital counter to measure period to .001 microsecond.

4.1.2 Test Procedure

The chamber was heated and cooled to temperatures of -65°, 10°, 85°, 160° and 200°F. At each temperature, the following pressures were applied: 25, 50, 100, 150, 200 and 250 psia.

At each of these test points, the following data were taken:

1. Pressure
2. Transducer temperature from thermocouple
3. Transducer diode voltage
4. Transducer period of vibration

Temperatures were set to within ±5°F with the environmental chamber controls, and after calibration the period at the exact temperature was found by interpolation on a curve of all the temperatures and periods measured at a given pressure.

4.1.3 Test Results

Initial tests showed that the transducer would vibrate normally up to 235°F but would not start reliably at this temperature and 250 psia, so calibration was carried out only up to 200°F.

In normal use, the transducers are corrected for temperature error or held at a fixed temperature, so it is necessary to incorporate a temperature sensor in each unit. The most convenient and accurate sensor for this purpose is a diode. This has an offset voltage sensitivity of about 1 millivolt per degree F, so it is 30 to 40 times as sensitive as a thermocouple and requires no cold junction or special lead wires. Also, its voltage is very linear with temperature. The one disadvantage for general use is that every diode must be individually calibrated. In this particular application, however, the calibration involves very little extra work since the transducers have to be calibrated at each temperature in any case. To avoid any error in converting from diode voltage to temperature to get temperature correction to period, the correction to period is recorded and applied directly in terms of diode voltage rather than temperature.

The test points corrected to exact reference temperature are shown on Table I. The diode voltage vs. temperature curve is shown in Figure 5. The exact values are tabulated in Table II. These can be used if it is ever desired to find transducer temperature from the diode output.

In Table I, Column 1 shows pressure. Column 2 shows the period of vibration in microseconds (t_0) when the transducer is at the reference temperature of 85°F.

Columns 3 to 7 show the correction (Δt) to the measured period (t). These column headings display both temperature and diode voltage, although the voltage is the variable actually used for correction as explained above. The Δt values are the corrections to be added to the measured period to get the corrected period listed in Column 2 at the pressure and temperature points listed.

The temperature correction at 250 psia and 200°F can be seen from Table I to be +.557. The period at the same pressure at 85°F from Column 2, last line, is 100.353. The corrected period for 200°F is then: 100.353 + .557 = 100.910.

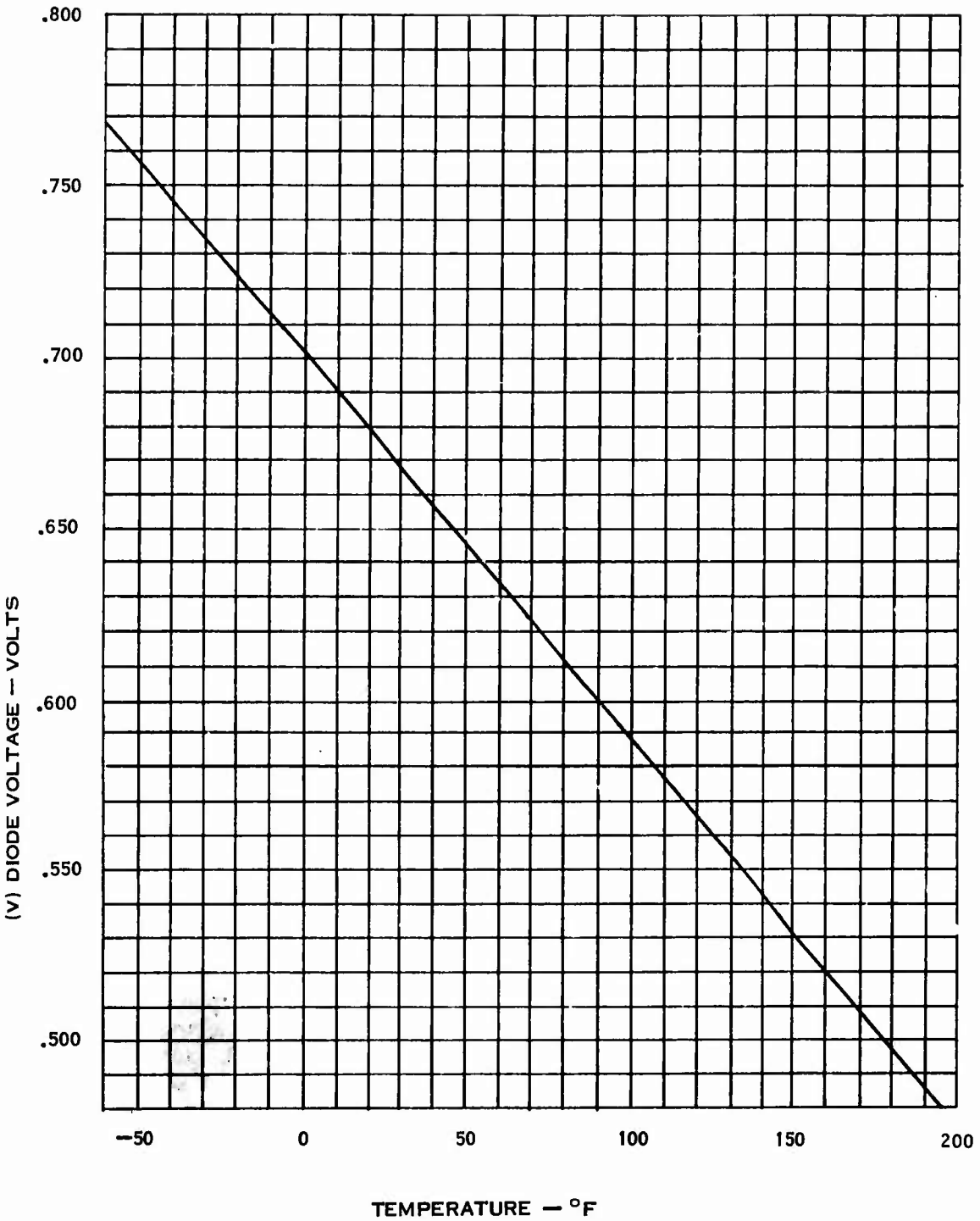

Figure 5. Temperature Diode Calibration.

TABLE I. PRESSURE TRANSDUCER CALIBRATION POINTS

Pressure Versus Period at 85°F		Temperature Correction (Δ t)				
(1)	(2)	(3)	(4)	(5)	(6)	(7)
Pressure (p)(psia)	Period (t_0) (μ sec)	T_f: -65°F V: .7722	10° F .6902	85° F .6055	160°F .5196	200°F .4758
1	145.636	+ .075	+.024	0	+.032	+.019
25	138.073	- .105	-.037	0	+.063	+.070
50	131.412	- .273	-.126	0	+.093	+.154
100	120.693	- .525	-.248	0	+.169	+.256
150	112.432	- .826	-.354	0	+.254	+.369
200	105.802	-1.073	-.448	0	+.317	+.483
250	100.353	-1.339	-.555	0	+.362	+.557

TABLE II. TEMPERATURE DIODE CALIBRATION

Temperature (°F)	Diode Voltage With 1 Milliampere Current
-65	.7722
10	.6902
85	.6055
160	.5196
200	.4758

In terms of percent full-scale values, it can be seen that the period range from 1 to 250 psia is 145.636 to 100.353 from Column 2, which gives a variation of 45.283. The correction of .557 is then 1.23% of full-scale signal or .0107% per degree F.

Figure 3 is a plot of Columns 1 and 2 in Table I.

Figure 6 shows how the temperature corrections are actually made. This is a plot of Columns 3-7 in Table I. When a given period and diode voltage are measured (t_a, E_a), five values of Δt can be calculated from the temperature curves as defined by diode voltages. The value of the correction Δt_a is then found by interpolating on this curve at the measured diode voltage, E_a.

The corrected period is

$$t_0 = t_a + \Delta t_a$$

This value of t_0 is used to enter the curve of Figure 3 to find pressure. Actually, the curve is not read directly since this would be too inaccurate, but the equation of the curve which is shown in Figure 3 is used to calculate p.

The equation of the curve is derived by computing a least-squares fit to a fourth-order polynomial equation to fit the points shown in Table I, Columns 1 and 2.

The temperature correction as illustrated in Figure 6 can be made graphically or from equations for the different temperature curves stored in a computer.

4.2 Voltage Sensitivity Calibration

At room temperature and 12, 15 and 18 volts input, the output frequency shift was measured at 1.5, 15 and 40 psia. The results are shown in Table III.

The maximum error is .0016% full scale at 1.5 psia and decreases with pressure. Since it requires a 3-volt variation from the nominal value of 15 volts, that is, a 20% variation to produce this error, the pressure error is only (1/12,500) as much as voltage variation.

This is in marked contrast to analog output transducers where errors are proportional to voltage variation.

In practice, voltage can easily be controlled to 1 volt, so for practical purposes, it can be said that normal live voltage variations give zero error.

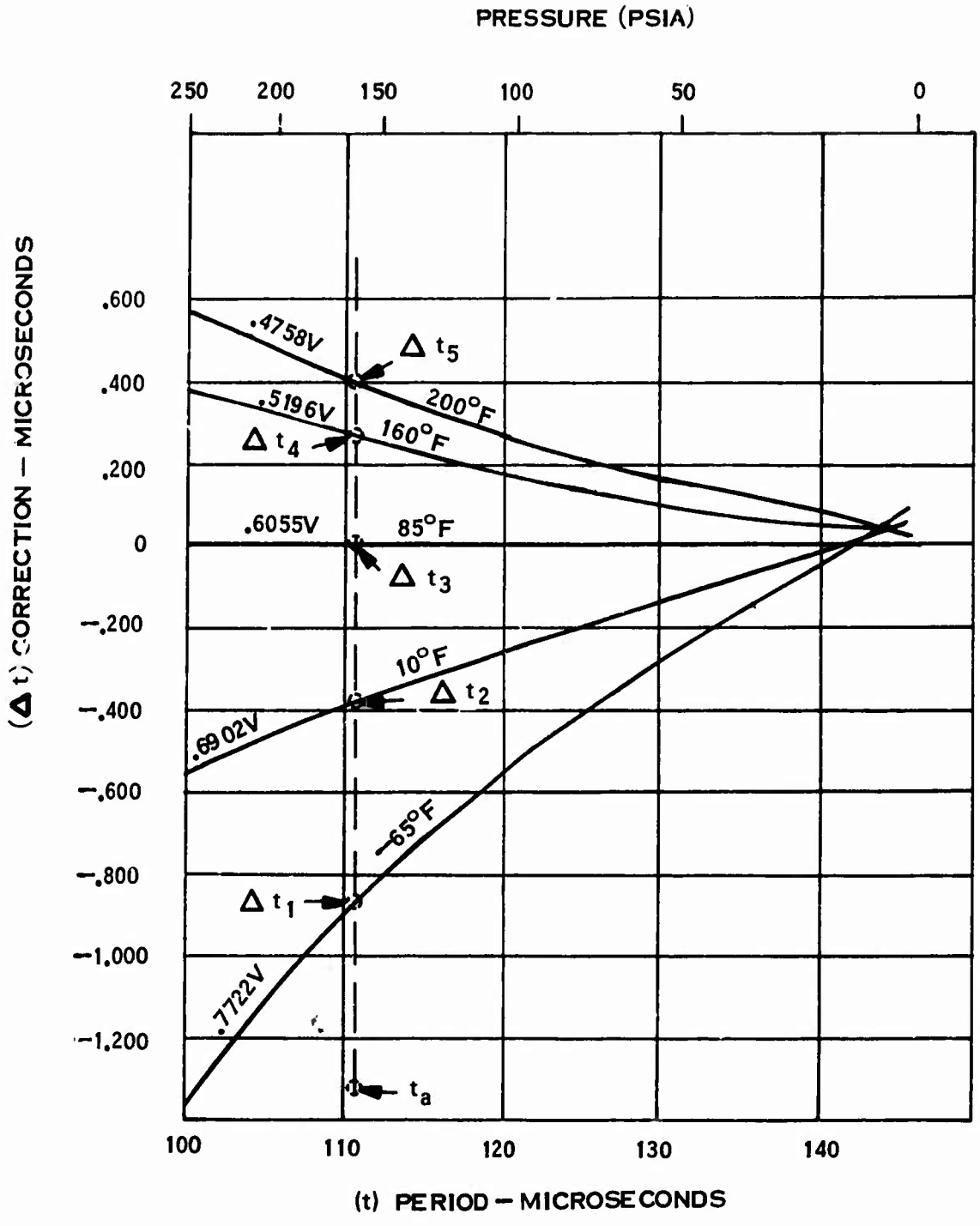

Figure 6. Temperature Correction.

TABLE III. VOLTAGE SENSITIVITY TEST RESULTS

Pressure (psia)	Voltage Deviation From 15V	% F.S. Error
1.5	-3	-.0016
	+3	+.0009
15	-3	-.0015
	+3	+.0015
40	-3	-.0010
	+3	+.0008

TABLE IV. ATTITUDE SENSITIVITY TEST RESULTS

Deviation for reversing orientation with respect to gravity for each axis (equivalent to 2g acceleration)

Pressure (psia)	X-Axis	Y-Axis	Z-Axis
1.5	0	0	.0007% F.S./2g
15	0	0	.0009
40	0	0	.0009

4.3 Acceleration and Attitude Sensitivity Calibration

At room temperature and 15 volts input, the frequency shift was measured at 1.5, 15 and 40 psia on each of the three orientations of the gravity axis. The results are shown in Table IV. These orientations are identified by the X, Y and Z axes being held respectively in a vertical position.

The X and Y axes are transverse to the cylinder; the X axis is parallel to the pressure port. The Z axis is parallel to the cylinder axis.

The transducer frequency was measured on each axis for two orientations 180° apart. The difference between these two readings is equal to a 2g acceleration along the vertical axis being tested. In one position, the g load is 1g positive; in the other position, it is 1g negative.

The results are expressed as percent full-scale errors for attitude reversal which is equivalent to 2 (F.S. error/g).

It can be seen that only the Z axis shows any error. This is due to the axial stress induced on the cylinder due to its own weight and amounts to .0004% full scale/g.

The practical immunity to acceleration and attitude errors demonstrated by this test is in contrast to flat diaphragm-type transducers, which are very sensitive to accelerations along the axis of the diaphragm. The immunity is created by the balanced mode of vibration in four sections radially symmetric about the cylinder axis and also by the vibrating principle where frequency of vibration is being measured rather than absolute diaphragm position.

4.4 Vibration Test

The transducer was vibrated on three axes at a 10g level from 10 to 10,000 Hz, and frequency errors were measured at resonance points.

4.4.1 Vibration Test Rig

The vibration test rig and associated equipment are shown in Figure 7. The test fixture for vibrating on the X and Y axes is shown in Figure 8.

For vibrating on the Z axis, the transducer was clamped directly to a parallel-sided mounting plate on the vibration table. For the other axes, it was mounted on the fixture, which is a solid aluminum block cut to fit the transducer base and to allow mounting with the axis horizontal. The vibration axis is vertical in all cases.

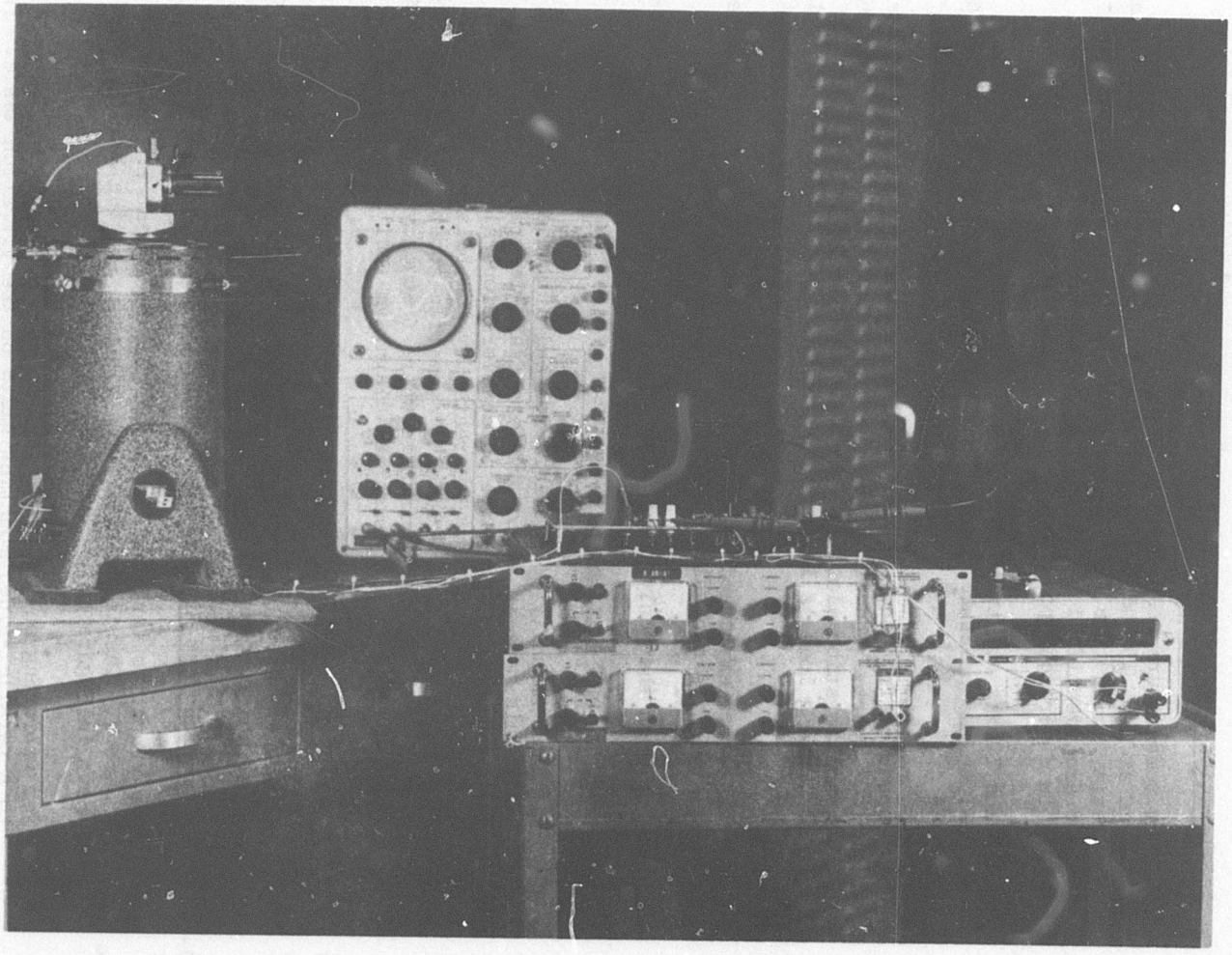

Figure 7. Vibration Rig.

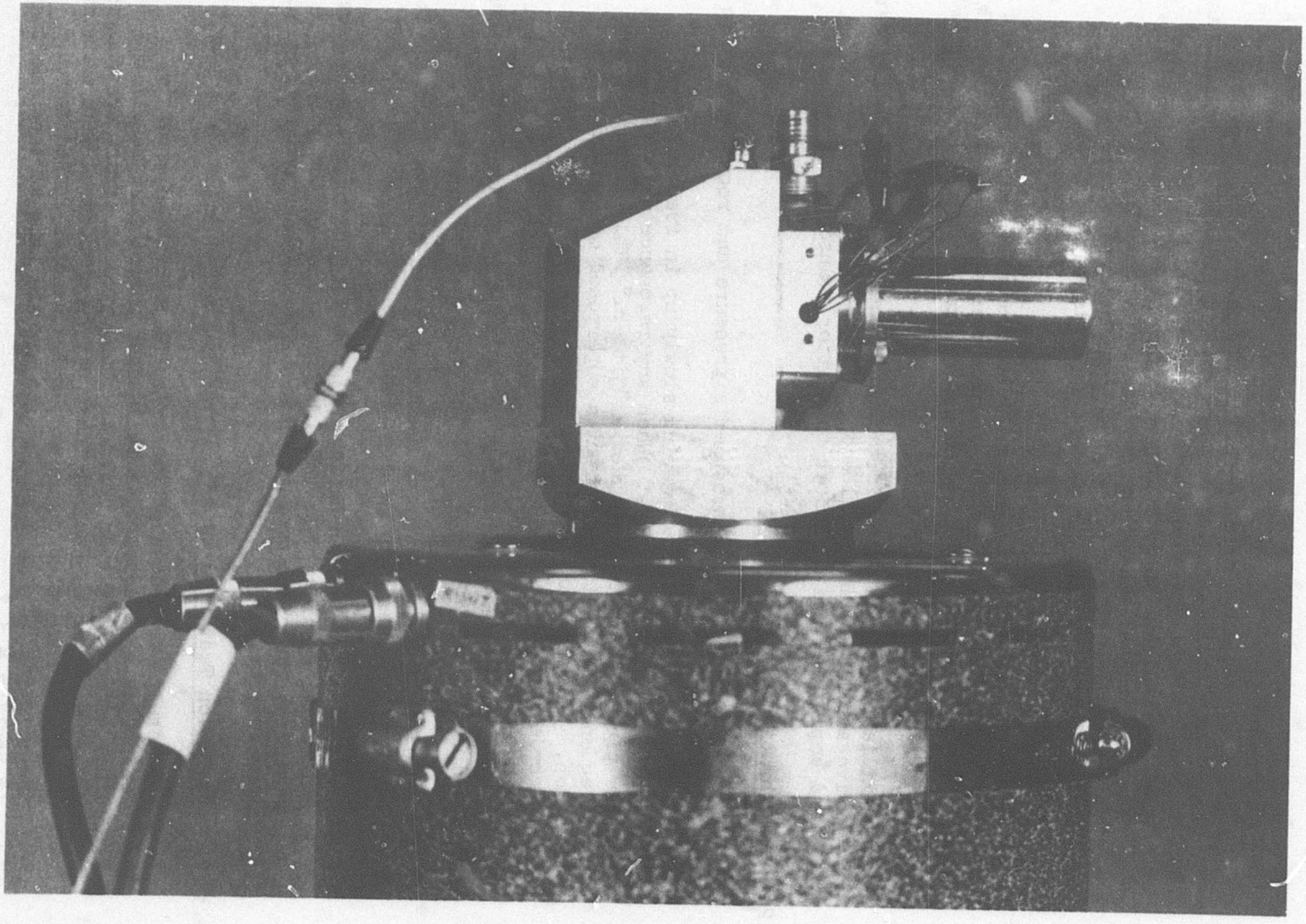

Figure 8. Vibration Test Fixture.

The test rig has an electromagnetic drive and is controlled by a variable-frequency, variable-amplitude power supply. A small accelerometer was mounted on the test fixture, and its output was used to control the amplitude. In operation, a g level is selected and maintained automatically by the accelerometer for all frequencies. The frequency can be varied manually by setting a dial, or it can be swept automatically up or down at a controlled rate. The frequency is displayed at all times on a large control dial.

The vibration rig has a natural resonance at about 8000 Hz, and no reliable measurements can be made over a span of about 500 Hz in this neighborhood, but otherwise it can be controlled from 10 to 10,000 Hz.

Auxiliary equipment used in the test consisted of the transducer drive amplifier, an oscilloscope to monitor pickup wave shape and amplitude, and a counter to monitor transducer period.

4.4.2 Vibration Test Procedure

All runs were made at atmospheric pressure and room temperature.

The tests were made by sweeping slowly up in frequency and watching the oscilloscope. When any resonance effect occurred, the pickup voltage would show a "jitter." This is due to the frequency modulation effect of a superposed mechanical vibration. When such an effect was noted, the period was read and recorded for ten counting periods, the maximum spread was measured, and one-half of this was recorded as the random vibration error since this represents the maximum deviation from true period due to vibration.

During the sweep, the period measurement was also monitored. It would vary normally by no more than one count from reading to reading and would change slowly with changes in atmospheric pressure. If a sudden shift in the reading occurred, more careful repeat readings were taken before and after the shift to determine the exact amount. This shift was then recorded as an offset error.

4.4.3 Vibration Test Results

The results are shown on Table V. The vibration error is defined as a percentage of full-scale output just as all the other errors have been defined. Two types of errors are shown: offset and random. Each of these can be associated with mechanical resonances which occur at the frequencies listed for the axes listed. The X, Y and Z axes are the same as those defined in Section 4.3.

TABLE V. VIBRATION TEST RESULTS
(Measured @ 10g)

Axis	Frequency (Hz)	% F.S. Offset Error	% F.S. Random Error
X	0-1800	0	.0002
	1800	.0012	.0002
	2100	.0093	.0002
	6800	0	.0005
	7200	0	.0009
	7500	0	.0007
	10000	0	.0018
Y	0-1800	0	.0002
	1800	.0009	.0002
	2100	.0080	.0002
	6700	0	.0006
	7100	0	.0009
	7500	0	.0009
Z	0-10000	0	.0002

The change in counter reading from zero to full pressure is 560,000, so a variation of one count is 1/560,000 or .0002 percent full scale (% F.S.).

Since the counter granularity is one count, the random error at all times will be .0002, and any additional random error due to mechanical vibration is added to this on a root sum square (RSS) basis.

Table V shows that errors on the X and Y axes are similar and occur at the same frequencies. Errors on the Z axis are zero (since the .0002% random error in this case is due to counter granularity).

The transducer has three cantilever structures: the pressure-sensing inner cylinder, the outer cylinder, and the spool body inside the inner cylinder which supports the electromagnets. For reasons given below, it would be expected that a vibration error can be incurred only by rocking of the pressure cylinder about its base or relative transverse displacement between the pressure cylinder and spool body due to vibration in the cantilever mode of one or both cylinders.

The test results confirm this conclusion. Since the cylinders are geometrically similar on the X and Y axes, they would be expected to behave identically for vibration on either axis. Vibration on the Z axis would not excite any cantilever vibration and hence has no effect on the transducer.

4.4.4 Theory of Random Vibration Errors

The normal vibration of the cylinder with no external vibration is sensed by an electromagnet transverse to the pressure cylinder axis. There are two air gaps in series with the magnet, and the cylinder vibration varies both gaps in the same sense simultaneously. This generates the output voltage. If the whole magnet assembly vibrates in a cantilever mode due to external vibration, one air gap will increase and the other decrease. Most of the net output is cancelled since these air gap variations induce bucking voltages, but there is a small net effect due to magnetic nonlinearity which generates a voltage at the vibration frequency.

Figure 9 shows the effect on the output voltage. Normally a timing signal is generated whenever the f_1 curve crosses the zero line. When the f_2 curve is added, its effect is to raise and lower the zero reference line. The circuit now senses the crossing point of the two curves as a zero crossing point ("measured zero crossing" in Figure 9), and this means that there is a trigger error of Δt.

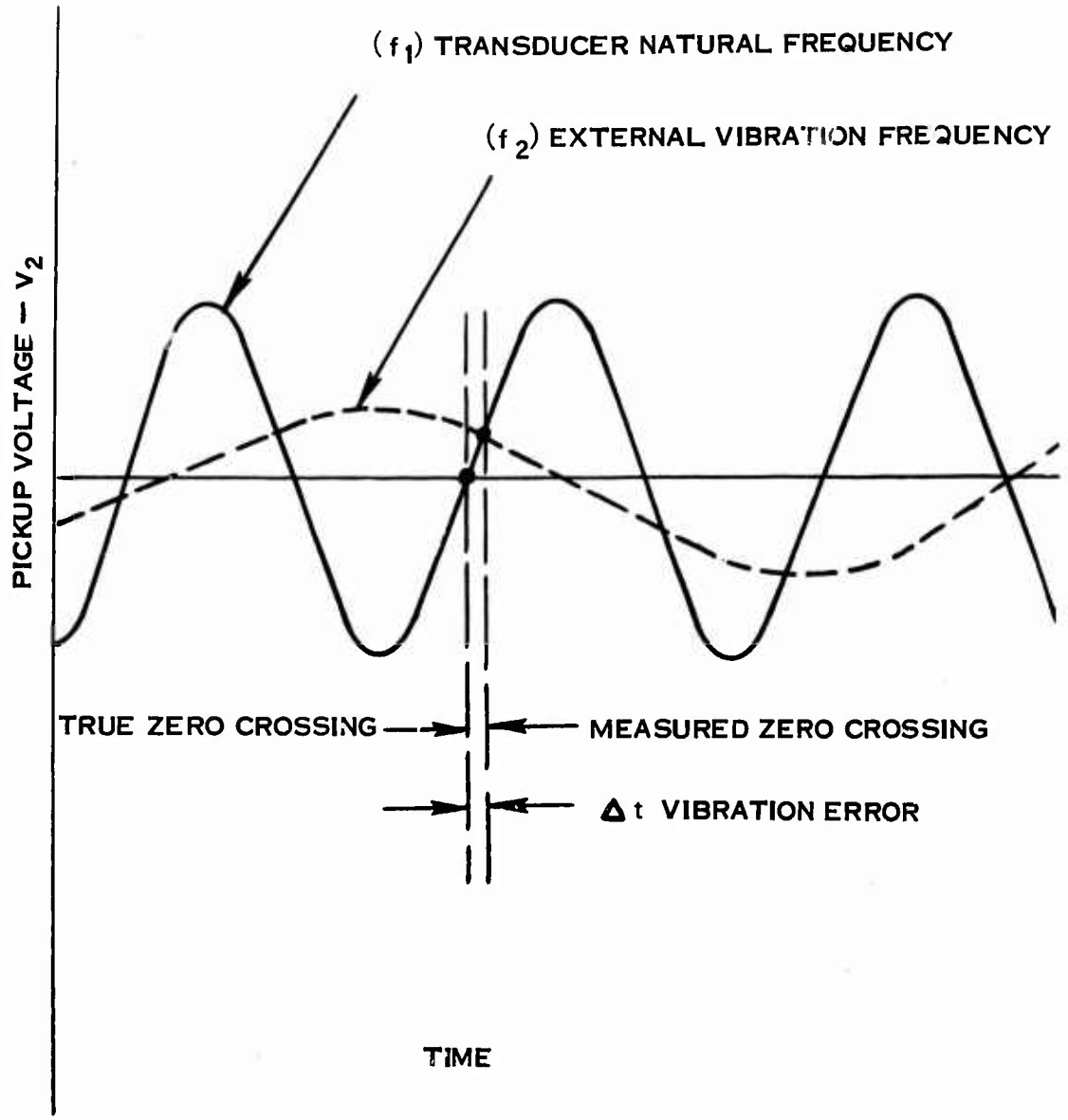

Figure 9. Vibration Error Diagram.

It can be seen that the Δt error is proportional to the f_2 amplitude at the cross-over point divided by the tangent of the angle at which the f_1 curve crosses the true zero axis.

The tangent of this angle increases with f_1 amplitude, so everything else being constant, Δt will decrease as signal strength (f_1 amplitude) increases.

In the case where f_2 is less than f_1 in amplitude, the maximum Δt error will occur when the phase relation between the two frequencies is such that f_2 is at a peak amplitude when f_1 is crossing the true zero axis. However, there is no fixed phase relationship between the two frequencies since they are completely independent of each other, so the Δt error can vary in a random way from one timing cycle to the next, from zero to a fixed maximum, which is determined by the maximum amplitude of both signals.

For the case where f_2 is greater than f_1 in amplitude, the primary signal is lost and output frequency becomes equal to mechanical resonance frequency. No case like this occurred during this particular test.

The error distribution curve for either case is non-Gaussian, so the ordinary rules of adding probable errors do not apply.

With a Gaussian distribution, errors can approach an infinite magnitude for a very small percent of the readings and no definite maximum error can readily be defined.

For this non-Gaussian case, however, the maximum error can readily be defined. Calculations showed that the average random error for a series of readings should be about one-half the maximum random error. Test data was evaluated which gave the same result. Since a relatively large percent of the readings are close to maximum error, it was concluded that the maximum spread in ten readings could be taken as a reliable measure of maximum error. Since the error can be either positive or negative, the spread represents twice the maximum error, so one-half this spread was taken as the random error as noted above.

For any error distribution, it can be shown that the probable timing error of a single reading can be reduced by timing more cycles. The counter gate can be constructed to time the period of any preselected number of cycles of f_1. If the number of cycles measured is n and the error is Gaussian, the probable error in percent would be $\Delta t/\sqrt{n}$, where Δt is the error for one cycle. For the error distribution in this case, the error is reduced in the ratio $\Delta t/n$. The period was measured with a 1-megacycle counter using a 10,000-cycle gate setting. The random error for any other number of counting cycles can be calculated

from this by multiplying by $(10{,}000/n_2)$, where n_2 is the number of cycles gated.

4.4.5 Theory of Offset Vibration Errors

The other effect of vibration is a change in the frequency of a fixed amount at a certain value of mechanical vibration frequency. This can be explained by the axial stress introduced by vibration in the cantilever mode. The cylinder frequency varies with both tangential and axial stress; pressure loading induces both kinds of stress. When the cylinder is rocking about its base, it is describing an arc of a circle. Its mean velocity tangent to a circle whose center is at the base will give a centrifugal loading that introduces an axial tension and raises the frequency.

This effect was noted at two frequencies and is larger in magnitude than the random errors. One peculiarity is that the random error was zero at these points, which indicates that the spool body and pressure tube were rocking in synchronism. Calculations indicate that both these members should have cantilever resonances at about 2000 Hz, so it is not impossible that both could be excited simultaneously; but to stay in phase, some other coupling would have to exist, and it is not clear what this mechanism could be.

4.4.6 Conclusions from Vibration Test

Mechanical vibrations above 2000 Hz are usually unimportant because normal transducer mountings on metal brackets act as shock absorbers above this frequency. In fact, the natural frequencies of small metal panels are usually of the order of 500 Hz.

It can be seen that the largest error, .0093% at 2100 Hz, occurs on the X axis, and a similar one of .0080% occurs on the Y axis.

This error is only .26 times the development target of .035% total error. If all the other errors amounted to e_1 = .035% and .26 e_1 is added on an RSS basis, the total error is increased to:

$$e_2 = .035\sqrt{1 + .26^2} = .035\ (1.032) = .036\%$$

This is a negligible increase, so it can be concluded that vibration error is negligible from 10 to 10,000 Hz at 10g.

Vibration errors are linearly related to g level, so the amount for other levels can be readily computed from Table V.

One of the development goals was to keep all vibration resonances above 1000 Hz, and this has been substantially exceeded.

5.0 TRANSDUCER ERRORS

The chief errors are:

1. Temperature
2. Gas Density (Composition)
3. Vibration
4. Acceleration
5. Voltage
6. Stability

These are all random errors, so they can be combined on a root sum square (RSS) as is derived from statistical theory to determine the overall error.

Temperature error as defined here is not the basic temperature effect on the frequency but a residual error after making a temperature correction. It was shown that transducer temperature is measured from the voltage offset of an internal diode, and this can be done to an accuracy of 0.1°F if the voltage is read to 0.1 millivolt. Because of temperature gradients and possible voltage errors, it is assumed that the accuracy of temperature measurement is 1°F. The random temperature error is then equal to the temperature deviation of frequency for 1°F change in temperature.

The RSS method of summing errors uses the equation

$$e_t = \sqrt{e_1^2 + e_2^2 + e_3^3 + \ldots}$$

where e_t = total error

e_1, e_2, etc. = individual errors

The units can be anything as long as they are the same for all items. In the discussion below, they are all in percent of full scale (% F.S.).

5.1 Temperature Error - e_1

Since this error is corrected on a first-order basis, the residual is equal to the error in the correction.

It might be thought that an additional error is introduced in the calibration of the diode itself. This was done with a thermocouple. But since the same diode was used for calibration, and since in use the correction can be thought of as being in terms of diode voltage rather than temperature and the corrections are plotted in terms of diode

voltage as well as temperature, the voltage should be used directly in using the curves rather than transforming them to temperature first.

The full-scale error in pressure for 1°F in temperature is calculated as follows:

The maximum error is at maximum pressure because the gas density is a maximum here and the temperature effect is chiefly a density effect.

This amounts to a total of 1.86 microseconds (Figure 3) for a temperature change of 265°F, or (1.86/265) = .007 μsec/°F.

The total change in period of the transducer from 0 to 250 psia is 45.2 microseconds (Table I), so the error is

$$e_1 = 100 \text{ X } (.007/45.2) = .015\% \text{ F.S.}$$

5.2 Gas Density Error - e_2

Anything that changes gas density changes the natural frequency of the cylinder. The effect of temperature changes on density are included in e_1. e_2 includes any error due to change in gas composition. For air, the only significant change is due to variations in humidity.

This error is calculated by taking typical air as having a mean humidity of 65% and a humidity range of 45 to 85% at 85°F.

This gives an air density change of ±0.40%.

From the temperature calibration curves in Figure 6, the density sensitivity of the transducer can be calculated as 5.7% of output signal, so the maximum humidity error is

$$e_2 = .057 \text{ X } .40 = .022\%$$

The transducer was calibrated with dry air, and the period versus pressure points were adjusted to track with 65% relative humidity. If the calibration is checked with a different gas, there will be changes in the period. For example, using nitrogen instead of air will give periods lower by as much as 0.25% at the same pressures and temperatures.

5.3 Vibration Error - e_3

Table V shows that there is no vibration error at 10g acceleration up to 1800 Hz, and the maximum above this is only .009% F.S. Since the target was vibration immunity up to 1000 Hz and this has been substantially exceeded, this error is considered zero.

$$e_3 = 0$$

5.4 g-Load Error - e_4

This is measured from the attitude tests. As shown in Table IV, this is zero except for the Z-axis. Normally, a transducer can be positioned to minimize this effect, but its maximum amount is included for 10g loading:

$$e_4 = 10 \times .00045 = .0045\% \text{ F.S.}$$

5.5 Voltage Error - e_5

This is a function of electrical design in use, but the pessimistic assumption is made of a possible 20% variation in voltage. The resulting error from Table III is

$$e_5 = \pm .0015\% \text{ F.S.}$$

5.6 Stability Error - e_6

The cylinder material is very stable mechanically and is stressed well below its micro-creep limit, so its stability on a long-term basis is very good.

A previous test on a low-pressure version of this transducer was made by recalibrating one transducer a year after its original calibration and after six months of pressure and temperature cycling. The measured points agreed within .015%, which was the rated accuracy of the pressure standards; hence there was no evidence of a change in calibration. But because of the uncertainty of the standards themselves, a figure of .015% is estimated; so

$$e_6 = .015\%$$

5.7 Total Error - e_t

The RSS total of the separate errors is

$$e_t = \sqrt{.015^2 + .022^2 + .0045^2 + .0015^2 + .015^2} = .031\%$$

which is less than the target figure of .035%.

5.8 Calibration Error

The errors listed above could be called the intrinsic errors of the transducer. They include all environmental effects, stability, and repeatability.

In addition to these, if the transducer is used to measure absolute pressure, there is an error in the reference standard itself.

For most transducers, the intrinsic errors are so much higher than those in the pressure standard that the latter can be considered zero. For this transducer, however, the intrinsic errors are comparable to the calibration error, so they should be separated.

The best available pressure standard at 250 psia is a deadweight gauge. This can have errors as low as .015%. The CEC gauge is rated at this value in the lower pressure range, and this was initially quoted as a typical value. However, further investigation showed that at 250 psia this gauge is rated at .025%. In addition, there is a frequency error inherent in the crystal clock of .001%.

The maximum frequency error on a full-scale basis is proportional to the absolute frequency error divided by the percentage of change in frequency over the operating range. In this case

$$(.001/.40) = .0025\% \text{ F.S.}$$

Combining these on an RSS basis gives

$$e_8 = \sqrt{.025^2 + .0025^2} = .0251\%$$

In other words, the crystal frequency error is negligible compared to the pressure gauge.

Taking the sum of the intrinsic errors plus the calibration error, the total RSS error for using the transducer to measure absolute measure is

$$et_2 = \sqrt{.031^2 + .025^2} = .040\%$$

6.0 CONCLUSIONS AND RECOMMENDATIONS

This development program has demonstrated the feasibility of extending the pressure range of the vibrating cylinder pressure transducer up to 250 psia. Auxiliary work done at Hamilton Standard has shown the feasibility of extending the temperature range up to 500°F.

It is recommended that further development be done to combine these two extensions in range. The immunity to vibration and attitude errors makes this type of transducer especially suitable for gas turbine measurements; and if the temperature and pressure ranges are extended, it could be mounted directly on a turbine and used to measure all the critical pressures.

APPENDIX

HAMILTON STANDARD DIVISION
HIGH-TEMPERATURE PRESSURE TRANSDUCER DEVELOPMENT PROGRAM

In accordance with the terms of the development contract, the results of a company-sponsored program to extend the operating temperature range of the vibrating cylinder transducer are summarized below.

The upper temperature limit of the current sensors is set by the deterioration in magnetic properties of the nickel-steel alloy above 200°F. This results in an absolute limit for magnetic excitation of about 265°F.

Sensors were constructed using high-temperature magnetic materials for the cylinders and high-temperature potting compounds and were operated as high as 490°F.

Although prolonged stability testing was not done, sensor output repeated accurately within the temperature range of -75°F to 490°F on a short-term basis. Their main difference from the low-temperature units is in the temperature correction curves.

The technique of minimizing the temperature effect has been explored analytically but has not yet been reduced to practice.